Feedback Regulation in the Lactose Operon: A Mathematical Modeling Study and Comparison with Experimental Data

Necmettin Yildirim* and Michael C. Mackey†
*Centre for Nonlinear Dynamics, McGill University, Montreal, Quebec, Canada H4X 2C1; and †Departments of Physiology, Physics and Mathematics, Centre for Nonlinear Dynamics, McGill University, Montreal, Quebec, Canada H4X 2C1

ABSTRACT A mathematical model for the regulation of induction in the *lac* operon in *Escherichia coli* is presented. This model takes into account the dynamics of the permease facilitating the internalization of external lactose; internal lactose; β-galactosidase, which is involved in the conversion of lactose to allolactose, glucose and galactose; the allolactose interactions with the *lac* repressor; and mRNA. The final model consists of five nonlinear differential delay equations with delays due to the transcription and translation process. We have paid particular attention to the estimation of the parameters in the model. We have tested our model against two sets of β-galactosidase activity versus time data, as well as a set of data on β-galactosidase activity during periodic phosphate feeding. In all three cases we find excellent agreement between the data and the model predictions. Analytical and numerical studies also indicate that for physiologically realistic values of the external lactose and the bacterial growth rate, a regime exists where there may be bistable steady-state behavior, and that this corresponds to a cusp bifurcation in the model dynamics.

INTRODUCTION

The operon concept (Beckwith, 1987b), introduced by Jacob et al. (1960), has had a profound and lasting effect on the biological sciences. Not long after the operon concept was developed, Goodwin (1965) gave the first mathematical analysis of operon dynamics. Griffith then put forward a more complete analysis of simple repressible (negative feedback, Griffith (1968a)) and inducible (positive feedback, Griffith (1968b)) gene control networks, and Tyson and Othmer (1978) have summarized these results. Extensions considering the stability of inducible operons were published by Selgrade (1979, 1982) and Ji-Fa (1994), but none of these treatments considered the role of the DNA transcription and mRNA translation delays, though Tyson and Othmer pointed out that both should be considered.

Bliss et al. (1982) were some of the first to explicitly consider transcriptional and translational delays in their modeling of the tryptophan operon. Many subsequent workers studying tryptophan dynamics (Sinha, 1988; Sen and Liu, 1989; Xiu et al., 1997) ignored these delays although including other biological details, but the tryptophan delays were considered by Santillán and Mackey, (2001a,b). Maffahy and Savev (1999) modeled *lac* operon dynamics and included transcriptional and translational delays, but Wong et al. (1997) failed to treat these elements of the *lac* operon despite their inclusion of much of the relevant biological detail. Recent work on gene network regulation can be found in Tyson and Mackey (2001).

Submitted October 10, 2002, and accepted for publication December 27, 2002.

Address reprint requests to Michael C. Mackey, 3655 Promenade Sir William Osler, Room 1124, Montreal, Quebec, Canada H3G 1Y6. Tel.: 514-398-4336; Fax: 514-398-7452; E-mail: mackey@cnd.mcgill.ca.

Necmettin Yildirim's permanent address is Atatürk Üniversitesi, Bilgisayar Bilimleri Uygulama ve Araştırma Merkezi, 25240 Erzurum, Turkey.

0006-3495/03/05/2841/11 $2.00

In this paper we offer a model of the induction process in the *lac* operon, including much of the relevant biological detail considered by Wong et al. (1997) (but neglecting catabolite repression) as well as the transcriptional and translational delays considered by Maffahy and Savev (1999). A more complete mathematical analysis of a reduced version of the model presented here is possible, and was considered by N. Yildirim, D. Horike, and M. C. Mackey (unpublished results). Section 2, ''The Model'', develops the model and gives a set of realistic parameters estimated from the biological literature (presented in detail in Appendix B). It also examines the nature of the steady states (as deduced in Appendix C) and briefly considers their stability (Appendix D). Section 3, ''Comparison with Experimental Data'', compares the numerical predictions of the model temporal behavior with three sets of data taken from the literature, and the paper ends with a discussion in Section 4, ''Conclusions''.

THE MODEL

To develop our model for regulation of the *lac* operon, it will be helpful to refer to Fig. 1. This control system functions in the following manner. In the absence of glucose available for cellular metabolism, but in the presence of external lactose (L_e), lactose is transported into the cell by a permease (P). Intracellular lactose (L) is then broken down into glucose, galactose, and allolactose (A) by the enzyme β-galactosidase (B). The allolactose feeds back to bind with the lactose repressor and enables the transcription process to proceed.

In more detail, the *lac* operon consists of a promoter/operator region and three larger structural genes, *lac*Z, *lac*Y, and *lac*A. Preceding the *lac* operon is a regulatory operon responsible for producing a repressor (R) protein. In the absence of allolactose (A), the repressor R binds to the operator region and prevents the RNA polymerase (which binds to the promoter region) from transcribing the structural genes. However, if allolactose is present, a complex is formed between allolactose and the repressor that makes binding of the repressor to the operator region impossible. In that case, the RNA polymerase bound to the promoter is able to initiate transcription of the structural genes to produce mRNA.

Once the mRNA has been produced, the process of translation is initiated.

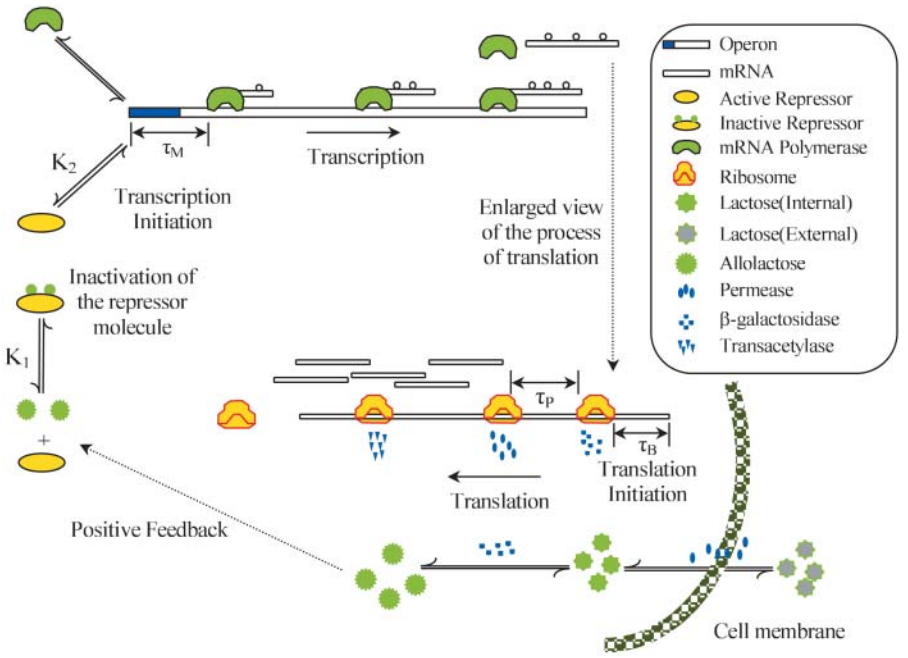

FIGURE 1 Schematic representation of the lactose operon regulatory system.

The *lac*Z gene encodes for the mRNA responsible for the production of β-galactosidase (B) and translation of the *lac*Y gene produces mRNA ultimately responsible for the production of a membrane permease (P). The mRNA produced by transcription of the *lac*A gene encodes for the production of thiogalactoside transacetylase, which is thought to not play a role in the regulation of the *lac* operon (Beckwith, 1987a) and will not be further considered here.

As shown in Appendix A, following Yagil and Yagil (1971), if the amount of repressor R bound to the operator O is small, then in a large population of cells the fraction of operators not bound by repressor (and therefore free to synthesize mRNA) is given by

$$f(A) = \frac{1 + K_1 A^n}{K + K_1 A^n}, \tag{1}$$

where n was interpreted as the number of molecules of allolactose required to inactivate the repressor, K_1 is the equilibrium constant for the repressor-allolactose reaction, and K_2 is the equilibrium constant for the operator-repressor reaction, $K = 1 + K_2 R_{tot}$, and R_{tot} is the total amount of repressor. Notice that there will be maximal repression when $A = 0$, but even at maximal repression there will still be a basal level of mRNA production (''leakage'') proportional to K^{-1}. We are now in a position to develop our model for the *lac* operon regulation.

The dynamics of mRNA production are given by Eq. 2,

$$\frac{dM}{dt} = \alpha_M \frac{1 + K_1 (e^{-\mu\tau_M} A_{\tau_M})^n}{K + K_1 (e^{-\mu\tau_M} A_{\tau_M})^n} + \Gamma_0 - \tilde{\gamma}_M M, \tag{2}$$

which is derived as follows. First, note that the production of mRNA from DNA via transcription is not an instantaneous process but requires a period of time, τ_M, for RNA polymerase to traverse the three structural genes. The rate of change of M is a balance between a production term $\alpha_M f$ and a loss term $\tilde{\gamma}_M M$. The argument of f in the production term is $e^{-\mu\tau_M} A_{\tau_M}$, where $A_{\tau_M} \equiv A(t - \tau_M)$, to account for the time, τ_M, required to produce the mRNA. The factor $e^{-\mu\tau_M}$ accounts for the growth dependent allolactose dilution during the transcriptional period. In the total absence of allolactose, on occasion repressor will transiently not be bound to the operator and RNA polymerase will initiate transcription. Γ_0 denotes this spontaneous rate of mRNA production. The loss term in Eq. 2, $\tilde{\gamma}_M M \equiv (\gamma_M + \mu)M$, is made up of an mRNA degradation term ($\gamma_M M$) and an effective loss due to dilution (μM).

The dynamics of β-galactosidase are described by Eq. 3,

$$\frac{dB}{dt} = \alpha_B e^{-\mu\tau_B} M_{\tau_B} - \tilde{\gamma}_B B. \tag{3}$$

Again realize that β-galactosidase production through mRNA translation is not instantaneous but requires a time, τ_B. We assume that the rate of production of B is proportional to the concentration of M a time τ_B ago ($\alpha_B e^{-\mu\tau_B} M_{\tau_B}$), where again the exponential factor takes into account the dilution of mRNA due to cell growth. The loss rate of B is given by $\tilde{\gamma}_B B$, where as before $\tilde{\gamma}_B = (\gamma_B + \mu)B$.

For the allolactose dynamics,

$$\frac{dA}{dt} = \alpha_A B \frac{L}{K_L + L} - \beta_A B \frac{A}{K_A + A} - \tilde{\gamma}_A A, \tag{4}$$

the first term in Eq. 4 gives the β-galactosidase mediated gain in allolactose from the conversion of lactose following the studies of Huber et al. (1976). The second term accounts for allolactose loss via conversion to glucose and galactose, again mediated by β-galactosidase (Martínez-Bilbao et al., 1991; Huber et al., 1994). The last term takes into account the degradation and dilution of allolactose.

The lactose dynamics are more complicated and given by Eq. 5:

$$\frac{dL}{dt} = \alpha_L P \frac{L_e}{K_{L_e} + L_e} - \beta_L P \frac{L}{K_{L_1} + L} - \beta_{L_2} B \frac{L}{K_{L_2} + L} - \tilde{\gamma}_L L. \tag{5}$$

The first term in Eq. 5 accounts for the augmentation of intracellular lactose L through the permease facilitated transport of L_e. The proportionality constant α_L is a decreasing function of extracellular glucose (Saier, 1976). The second term deals with intracellular lactose loss to the extracellular fluid because of the reversible nature of the permease-mediated transport (Saier, 1976; Osumi and Saier, 1982; Postma et al., 1996; Saier et al., 1996). The coefficient β_L is not dependent on the external glucose levels. The third term accounts for the conversion of lactose to allolactose as well as the hydrolysis

of lactose to glucose and galactose via β-galactosidase (B). The fourth term accounts for the decrease in internal lactose concentration due to degradation and dilution.

To describe the permease dynamics

$$\frac{dP}{dt} = \alpha_P e^{-\mu(\tau_P+\tau_B)} M_{\tau_P+\tau_B} - \tilde{\gamma}_P P \tag{6}$$

we have Eq. 6. There, the first term reflects the assumption that permease production is directly proportional (proportionality constant α_P) to the mRNA concentration a time ($\tau_P + \tau_B$) in the past, where τ_P is the translation time between mRNA and permease. The delay is taken to be the sum of the β-galactosidase and permease translation times under the assumption that permease production cannot start until β-galactosidase production is complete. The exponential factor $e^{-\mu(\tau_P+\tau_B)}$ accounts for dilution of mRNA concentration due to cell growth. The second term accounts for the degradation and dilution of permease.

We have carried out an extensive search of the existing literature for data that would allow us to estimate the model parameters in Eqs. 2–6. The results of our determinations are summarized in Table 1, and the details of how we arrived at these parameter values are contained in Appendix B.

The full model as formulated in Eqs. 2–6 can have one, two, or three steady states depending on the values of the parameters (μ, L_e). The details of how these steady states are determined are contained in Appendix C. The results of these considerations are presented in Fig. 2. There we show in $(L_e, \bar{A})$ space the region where a nonnegative steady state can exist. Note in particular that for a range of L_e values, there may be three coexisting steady-state values of the intracellular allolactose levels, $\bar{A}$ and, consequently, of $(\bar{M}, \bar{B}, \bar{A}, \bar{L}, \bar{P})$.

Whether or not there can be coexisting steady states depends on the growth rate μ, and an examination of the dependence of the criteria for the existence of steady states $(\bar{M}, \bar{B}, \bar{A}, \bar{L}, \bar{P})$ on (μ, L_e) reveals that in $(\mu, L_e, \bar{A})$ space there is a cusp bifurcation occurring that is dependent on the growth rate μ and extracellular lactose levels L_e.

This cusp bifurcation in the model in $(\mu, L_e, \bar{A})$ space is of the following nature. There is a minimal growth rate $\mu_{min} \simeq 4.5 \times 10^{-3}$ min^{-1} such that for values of the growth rate $\mu \in [0, \mu_{min}]$, there is a unique steady-state level of allolactose $\bar{A}$ for any given value of external lactose levels L_e. At $\mu = \mu_{min}$, the concentration of external lactose required for induction is $L_e \simeq 4.5\,\mu$M. However, as μ becomes larger, $\mu \in [\mu_{min}, \mu_{max}$, the system may have three steady-state values of $\bar{A}$ at a given external lactose level L_e. This is the situation depicted in Fig. 2, where we used $\mu = \bar{\mu} = 2.26 \times 10^{-2}$ min^{-1}. For this value of μ, the lactose concentration required for induction (and marked with an asterisk in Fig. 2) is $L_e \simeq 62\,\mu$M, which compares well with the results of a study using an artificial inducer of the *lac* operon, isopropylthiogalactoside (IPTG) (Baneyx, 1999). There it was found that 50–100 μM IPTG is sufficient as a lower bound to achieve full induction.

A full stability analysis of the steady states of this model is impossible, since the eigenvalue equation determining local stability is a fifth order quasipolynomial containing three delays. Consequently, we have contented ourselves with a numerical examination of the stability properties of the steady states. Briefly, the results of our numerical stimulations presented in Appendix D are as follows. When a single steady state exists, we have found that the numerical behavior is such that the model solutions always converge to that steady state at large times. When there are three coexisting steady states, the numerical solutions to the model either converged to the lower or upper branch of the S-shaped curve for various initial conditions. These results, as well as numerous others that are not shown, lead us to conclude that the middle branch of the S-shaped steady-state curve (see Fig. 2) corresponds to a steady state that is globally unstable. The nature of the boundary between initial conditions leading to the convergence to the upper or lower branch solution appears to be complicated, and it may well be a fractal basin boundary (Losson and Mackey, 1993).

TABLE 1 The estimated parameters for the model as determined in Appendix B

n	2	μ_{max}	3.47×10^{-2} min^{-1}
γ_M	0.411 min^{-1}	γ_B	8.33×10^{-4} min^{-1}
γ_A	0.52 min^{-1}	Γ_0	7.25×10^{-7} mM/min
K	7,200	α_M	9.97×10^{-4} mM/min
τ_B	2.0 min	α_A	1.76×10^{4} min^{-1}
K_{L1}	1.81 mM	α_B	1.66×10^{-2} min^{-1}
K_A	1.95 mM	β_A	2.15×10^{4} min^{-1}
τ_M	0.1 min	K_L	9.7×10^{-4} M
γ_L	0.0 min^{-1}	γ_P	0.65 min^{-1}
α_L	2880 min^{-1}	α_P	10.0 min^{-1}
τ_P	0.83 min	β_{L1}	2.65×10^{3} min^{-1}
K_{Le}	0.26 mM	K_1	2.52×10^{-2} (μM)$^{-2}$

COMPARISON WITH EXPERIMENTAL DATA

Given the parameter values determined in Table 1, we numerically solved the model equations to compare the predicted behavior with three distinct experimental data sets.

The first data set is from Knorre (1968), in which changes of the specific β-galactosidase concentration after a step change from glucose to lactose growth for *Escherichia coli* ML30 were measured. The second data set is from Pestka et al. (1984). In this paper, Pestka et al. studied specific inhibition of translation of single mRNA molecules and gave data for the specific activity of β-galactosidase versus time for *E. coli* 294 in the presence of IPTG. These two data sets and the model simulation determined using MATLAB's dde23 (Shampine and Thompson, 2000) routine are shown in Fig. 3.

For this simulation, initial values for the variable were chosen as $A_0 = 3.80 \times 10^{-2}, M_0 = 6.26 \times 10^{-4}, L_0 = 3.72 \times 10^{-1}$, $P_0 = 1.49 \times 10^{-2}$, and $B_0 = 0.0$ mM, all of which are close to the steady-state values given in Table 2 when $L_e = 8.0 \times 10^{-2}$ mM. (With this value of L_e, there is a single unique steady state). To compare these two sets of experimental data with the model simulation predictions, the data were scaled so the steady-state values of measured β-galactosidase activities and those produced by the simulation were equal. As seen in Fig. 3, there is relatively good agreement between both sets of experimental data and the model-predicted temporal approach of β-galactosidase activity to its steady-state value.

As a third test of the model, a data set from Goodwin (1969) was used. In this paper, the dynamic behavior of β-galactosidase was studied in chemostat cultures of *E. coli* synchronized with respect to cell division by periodic phosphate feeding at a period equal to the bacterial doubling time. Experimentally, oscillations in β-galactosidase concentration were observed with a period equal to the feeding period.

To mimic the periodic phosphate feeding in our simulation, we assumed that the bacterial growth rate varies as a function of time in manner given by

$$\mu(t) = \bar{\mu} - \alpha \,\mathrm{mod}(t, \mathrm{T}). \tag{7}$$

Here, $\bar{\mu}$ is the maximal growth rate for the bacteria, T is the period of the feeding and α is a positive parameter with

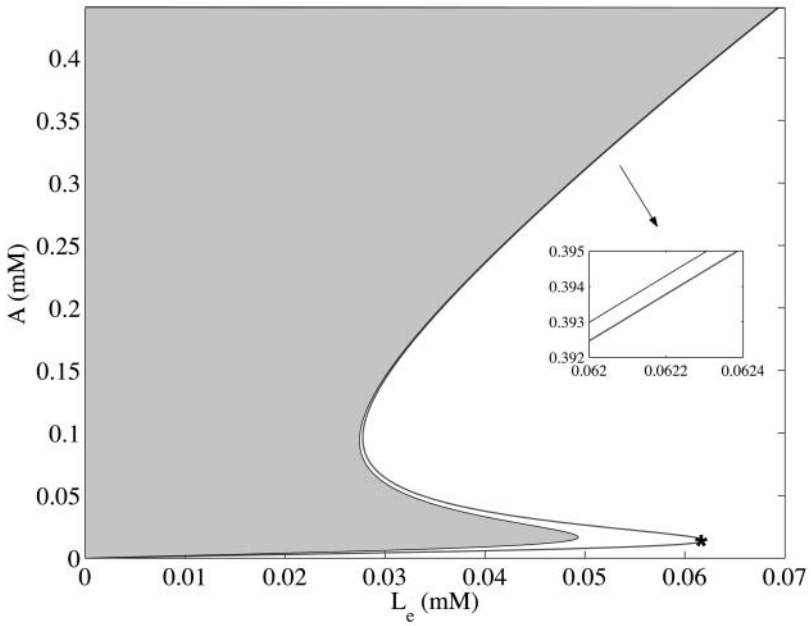

FIGURE 2 The region in the $(L_e, \bar{A})$ space where a nonnegative steady state can exist as a function of external lactose levels L_e for the model when all parameters are held at the estimated values in Table 1 and when $\bar{\mu} = 2.26 \times 10^{-2}\,\mathrm{min}^{-1}$. The shaded area shows the region where a steady state is not defined, whereas the solid line is the locus of $(L_e, \bar{A})$ values satisfying the steady state. The inset box shows that at large values of L_e, there is still a separation of the line for the steady state from the region where steady states are not defined. Notice that for these values of the parameters, there is a range of L_e values for which there are three coexisting steady-state values of allolactose A. The asterisk located at the right-most kink locates the minimal concentration of extracellular lactose required for induction, and our calculations indicate that it should be on the order of 62.0 μM.

dimension min^{-2}. mod(t, T) is a function that gives the remainder on division of t by T. Selection of this type of function is motivated by the observation that growth rates decrease as nutrient levels fall and sharply increase after the addition of nutrient.

$\mu(t)$ takes its maximal value of $\bar{\mu}$ when $t = \mathrm{T} \times k$, ($k = 1, 2, 3, \ldots$), which corresponds to the times that phosphate was added. The minimal value of this function, $\bar{\mu} - \alpha(\mathrm{T} - \varepsilon)$ at $t = \mathrm{T} \times k - \varepsilon$, ($\varepsilon \geq 0$, $k = 1, 2, 3, \ldots$), represents the minimal amount of nutrient left in the vessel. Assuming no nutrient is left ε minutes before the addition of phosphate and letting $\varepsilon \to 0$, α can be estimated if the doubling time (T) is known: $\alpha \simeq \bar{\mu}/T$.

With a feeding period of $T = 100$ min, we have $\alpha \simeq 2.26 \times 10^{-4}\,\mathrm{min}^{-2}$ for $\bar{\mu} = 2.26 \times 10^{-2}\,\mathrm{min}^{-1}$, which is the value we have estimated for our model (cf. Appendix B). In Fig. 4, we compare the data on β-galactosidase activity from the forced culture as a function of time with the model predictions.

With respect to the predicted bistability at sufficiently large growth rates, illustrated in Fig. 2, evidence presented by Novick and Wiener (1957) and Cohn and Horibata (1959) qualitatively substantiate the existence of this behavior for values of the growth rate exceeding $\mu_{\min}$. However, we are unable to determine if the quantitative ranges of L_e for which we have predicted bistability correspond to the conditions under which it was seen in Novick and Wiener (1957) and Cohn and Horibata (1959).

CONCLUSIONS

Here we have developed, and analytically and numerically analyzed, a mathematical model for the regulation of the *lac* operon in *E. coli*. The final model consists of five nonlinear differential delay equations with delays due to the DNA transcription and mRNA translation processes. The model equations describe the dynamics of the permease (P) facilitating the internalization of external lactose (L_e); internal lactose (L); β-galactosidase (B), which is involved in the conversion of lactose to allolactose, glucose, and galactose; the allolactose (A) interactions with the *lac* repressor, and mRNA (M). We have gone to considerable effort to make valid and reasonable estimates of the 24 parameters in the model. We were successful in identifying 22 of these parameters from published data, but were forced to determine the growth rate μ and γ_A by fitting the model to the data of Knorre (1968).

We have tested our model against two sets of β-galactosidase activity versus time data. These data came from the experimental work presented in Knorre (1968), in which changes of the specific β-galactosidase concentration after a step change from glucose to lactose growth for *E. coli* ML30 were measured, and the work of Pestka et al. (1984). In this latter paper, data were presented for the specific activity of β-galactosidase versus time for *E. coli* 294 in the presence of IPTG. These two data sets and the model simulation are shown in Fig. 3, and there is a remarkable degree of concordance between the data and the model predictions.

As a third test of the model, data from Goodwin (1969) giving the dynamic behavior of β-galactosidase was studied in chemostat cultures of *E. coli* synchronized with respect to cell division by periodic phosphate feeding at a period equal to the bacterial doubling time. Experimentally, oscillations in β-galactosidase concentration were observed with a period equal to the feeding period. Fig. 4 shows the β-galactosidase activity data as well as the model predictions. Again, there is a satisfying degree of agreement.

Analytical and numerical studies of the model also predict

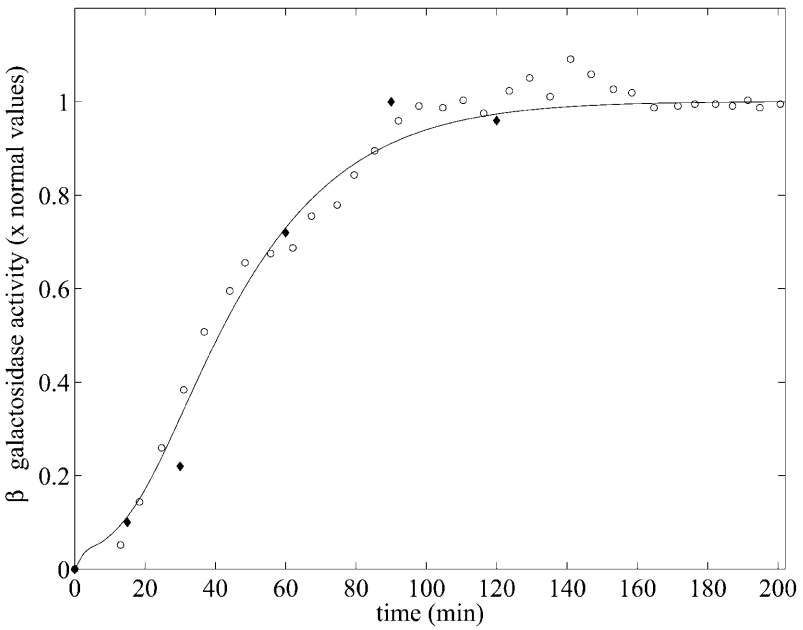

FIGURE 3 β-galactosidase activity versus time when $L_e = 8.0 \times 10^{-2}$ mM. The experimental data sets were taken from Knorre (1968) for *E. coli* ML30 (○) and from Pestka et al. (1984) for *E. coli* 294 (♦). The model simulation (*solid line*) was obtained using the parameters of Table 1 with a growth rate $\bar{\mu} = 2.26 \times 10^{-2}$ min^{-1}. The selection of initial conditions is described in the text.

that for physiologically realistic values of external lactose and the bacterial growth rate, a regime exists where there may be bistable steady-state behavior, and that this corresponds to a cusp bifurcation in the model dynamics. This prediction is qualitatively confirmed by the observations of Novick and Wiener (1957) and Cohn and Horibata (1959). Although a full analysis of the stability properties of the model is not possible due to its complexity, we have found that the basic properties contained in a reduced version of this model N. Yildirim, D. Horike, and M. C. Mackey (unpublished results) (2002) (which considered only the dynamics of M, B, and A) are apparently retained in this much more complicated model as far as we are able to ascertain analytically and numerically.

This agreement between the model predictions for the lactose operon and existing data, and similar agreement between a mathematical model for the tryptophan operon (Santillán and Mackey, 2001a,b), highlight the desirability and necessity of closer cooperation between experimentalists and modelers to further validate and refine mathematical models of simple and more complicated gene regulatory networks.

To close, we wish to touch on the nature of the mathematical model presented here. The model considered in this paper is formulated with the explicit assumption that one is dealing with large numbers cells (and hence of large numbers of molecules) so that the law of large numbers is operative. However, the situation is quite different if one is interested in the dynamics of small numbers (or single) prokaryotic or eukaryotic cells, for then the numbers of molecules are small. Adequate means to analytically treat such problems do not exist in a satisfactory form as of now (Gillespie, 1992; Kepler and Elston, 2001; Swain et al., 2002), and one is often reduced to mostly numerical studies (Gillespie, 1977; McAdams and Shapiro, 1995; Arkin et al., 1998). The situation is analogous to examining the interactions between small numbers of interacting particles (where the laws of mechanics or electrodynamics hold), and then deriving from these formulations the behavior of large numbers of identical units as is done (not completely successfully even at this point) in statistical mechanics. We view this connection between the ''micro'' and ''macro'' levels as one of the major mathematical challenges facing those interested in the understanding of gene control networks.

TABLE 2 Steady-state values when $L_e = 8.0 \times 10^{-2}$ mM

$\bar{A} = 5.06 \times 10^{-1}$ mM
$\bar{M} = 1.08 \times 10^{-3}$ mM
$\bar{B} = 7.35 \times 10^{-4}$ mM
$\bar{L} = 3.64 \times 10^{-1}$ mM
$\bar{P} = 1.51 \times 10^{-2}$ mM

APPENDIX A: REPRESSOR DYNAMICS

Let R be the repressor, E the effector (allolactose in our case), and O the operator. The effector is known to bind with the active form R of the repressor. We assume, as do Yagil and Yagil (1971), that this reaction is of the form

$$R + nE \overset{K_1}{\rightleftharpoons} RE_n \quad K_1 = \frac{RE_n}{R \cdot E^n}, \tag{8}$$

where they took n to be the effective number of molecules of effector required to inactivate the repressor R. Furthermore, the operator O and repressor R are assumed Yagil and Yagil (1971) to interact according to

$$O + R \overset{K_2}{\rightleftharpoons} OR \quad K_2 = \frac{OR}{O \cdot R}. \tag{9}$$

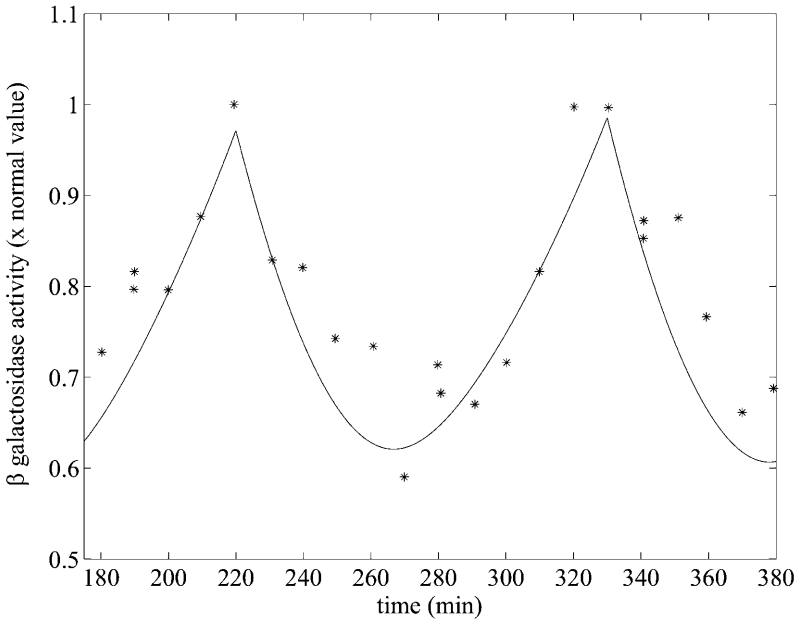

FIGURE 4 Oscillation in β-galactosidase activity in response to periodic phosphate feeding with period $T = 100$ min, which is the culture doubling time. The experimental data (*) together with the model simulation (*solid line*) using the parameters of Table 1 and $\bar{\mu} \simeq 2.26 \times 10^{-2}$ min^{-1} are presented. The experimental data are taken from Goodwin (1969). In the numerical simulation, periodic phosphate feeding was imitated by choosing a periodic function given by Eq. 7. The simulation was calculated by numerically solving the system of delay differential equations given by Eqs. 2–6. The initial conditions are the same as those values given in Table 2 for $L_e = 8.0 \times 10^{-2}$ mM.

Let the total operator be O_{tot}:

$$O_{tot} = O + OR = O + K_2 O \cdot R = O(1 + K_2 R), \qquad (10)$$

and the total level of repressor be R_{tot}:

$$R_{tot} = R + K_1 R \cdot E^n + K_2 O \cdot R. \qquad (11)$$

The fraction of operators not bound by repressor (and therefore free to synthesize mRNA) is given by

$$f(E) = \frac{O}{O_{tot}} = \frac{1}{1 + K_2 R}. \qquad (12)$$

If the amount of repressor R bound to the operator O is small

$$R_{tot} \simeq R + K_1 R \cdot E^n = R(1 + K_1 E^n) \qquad (13)$$

so

$$R = \frac{R_{tot}}{1 + K_1 E^n}, \qquad (14)$$

and consequently

$$f(E) = \frac{1 + K_1 E^n}{1 + K_2 R_{tot} + K_1 E^n} = \frac{1 + K_1 E^n}{K + K_1 E^n}, \qquad (15)$$

where $K = 1 + K_2 R_{tot}$. Notice that there will be maximal repression when $E = 0$ but even at maximal repression there will still be a basal level of mRNA production proportional to K^{-1}.

APPENDIX B: PARAMETER ESTIMATION

In the model given by Eqs. 2–6, there are 24 parameters in total that must be estimated to characterize the system completely. In this section, we give the estimation of each of these parameters.

μ: The maximal value of the dilution rate μ can be estimated from the shortest interdivision time of *E. coli*, which is ~20 min (Watson, 1977). Given this, $\mu_{max} = \ln 2/20$ min^{-1} $= 3.47 \times 10^{-2}$ min^{-1}. We have also estimated a value of μ, denoted by $\bar{\mu}$, together with the value of γ_A by least-square fitting of the experimental β-galactosidase concentration data given in Knorre (1968) using the fminsearch and dde23 (Shampine and Thompson, 2000) routines in MATLAB. We found $\bar{\mu} \simeq 2.26 \times 10^{-2}$ min^{-1}, indicating that these cultures were growing with a doubling time of 30 min. The results of this estimation were tested for several initial starting points for μ and γ_A, and the estimation procedure always converged to the same values of $\bar{\mu}$ and γ_A.

γ_A: The value of γ_A was estimated as 5.2×10^{-1} min^{-1} together with the value of μ by using least-square fitting of the experimental β-galactosidase activity data given in Knorre (1968) as above.

γ_M: Leive and Kollin (1967) found that the $t_{1/2}$ of β-galactosidase mRNA was 2 min to give a value of $\gamma_M \simeq \ln 2/2 = 0.347$ min^{-1}. In a comparable experiment, Blundell and Kennell (1974) found $t_{1/2} = 1.47$ min to give $\gamma_M \simeq 0.475$ min^{-1}. We have taken the average of these two figures to give $\gamma_M \simeq 0.411$ min^{-1}.

γ_B: The rate of breakdown of β-galactosidase was measured by Mandelstam (1957) and found to be 0.05 per h corresponding to 8.33×10^{-4} min^{-1}. Rotman and Spiegelman (1954) also reported that the maximal rate of breakdown of β-galactoside is 0.005 min^{-1}, and noted that it is possibly much smaller than this value. We have taken the Mandelstam value.

K: Yagil and Yagil (1971) analyzed a number of published data sets, and from their calculations we find the average value is $K \simeq 7200$.

n: Again from Yagil and Yagil (1971), we have an average Hill coefficient of 2.09. We have taken $n = 2$.

K_1: The average dissociation constant of effector-repressor complex was $K_1 \simeq 2.52 \times 10^{-2} (\mu M)^{-2}$ from the results of Yagil and Yagil (1971).

α_M: The steady-state value of *lac* mRNA in the absence of induction is thought to be one molecule per cell. This corresponds to a "concentration" of 2.08×10^{-6} mM if we take the *E. coli* volume to be 8×10^{-16} liter. When the cells are maximally induced, the *lac* mRNA level is raised a thousand times compared to this uninduced steady-state value (Savageau, 1999). From Eq. 2 at a steady state,

$$\lim_{\bar{A} \to 0} \Gamma_0 = \tilde{\gamma}_M \bar{M} - \frac{\alpha_M}{K} \qquad (16)$$

$$\lim_{\bar{A}\to\infty}\Gamma_0 = \tilde{\gamma}_M 1000\bar{M} - \alpha_M. \quad (17)$$

From Eqs. 16 and 17, α_M is 9.97×10^{-4} mM–min^{-1}.

Γ_0: The term Γ_0 was included in our model for the following reason. Assume that the term in question is not there, which is equivalent to taking $\Gamma_0 \equiv 0$. An examination of Eq. 2 in a steady state yields $\alpha_M f(\bar{A}e^{-\mu\tau_M}) = \tilde{\gamma}_M\bar{M}$. Let the level of lac mRNA in the maximally induced state be given by $\bar{M}_{maxinduced} = \Theta\bar{M}_{uninduced}$. The maximally induced state corresponds to $\bar{A} \to \infty$ and $\lim_{\bar{A}\to\infty} f(\bar{A}e^{-\mu\tau_M}) = 1$. The uninduced state corresponds to $\bar{A} \to 0$ and $\lim_{\bar{A}\to 0} f\,(\bar{A}e^{-\mu\tau_M}) = 1/K$. Thus we have two relations,

$$\tilde{\gamma}_M\bar{M}_{maxinduced} \equiv \tilde{\gamma}_M\Theta\bar{M}_{uninduced} = \alpha_M$$

and

$$\tilde{\gamma}_M\bar{M}_{uninduced} = \frac{\alpha_M}{K}.$$

Taking the ratio of these two relations gives $\Theta \equiv K$ and from above, $K = 7200$, which would imply a value for Θ which is 7.2 times larger than what is experimentally observed ($\Theta = 1000$). Thus the inclusion of the term Γ_0.

To determine Γ_0, note that at a steady state when $\bar{A} \simeq 0$, from Eq. 2 we have

$$\Gamma_0 = \tilde{\gamma}_M\bar{M} - \frac{\alpha_M}{K} = 7.25 \times 10^{-7}\,\text{mM}\,\text{min}^{-1}.$$

α_B: At a steady state, from Eq. 3 we have

$$\alpha_B = \frac{\tilde{\gamma}_B\bar{B}}{\bar{M}}e^{\mu\tau_B}. \quad (18)$$

Kennell and Reizman (1977) reported that steady-state value of β-galactosidase is ~20 molecules per cell, which means that $\bar{B}/\bar{M} = 20$. Using the value of γ_B reported by Mandelstam (1957) for nongrowing bacteria, $\alpha_B \simeq 1.66 \times 10^{-2}$ min^{-1}.

α_A: Huber et al. (1975) studied the kinetics of β-galactosidase and found $V_{max} = 32.6$ U/mg of β-galactosidase and $K_M = 0.00253$ M when lactose was the substrate. whereas $V_{max} = 49.6$ U/mg of β-galactosidase and $K_M = 0.00120$ M when allolactose is the substrate. (U is defined as μM of glucose or galactose produced per minute.) Given that the molecular mass of β-galactosidase is 540,000 Da, and 1 Da $= 1.66 \times 10^{-21}$ mg, 1 mol of β-galactosidase is equivalent to $6.02 \times 10^{23} \times 5.4 \times 10^5 \times 1.66 \times 10^{-21} = 5.39 \times 10^8$ mg of β-galactosidase, so 1 mg of β-galactosidase is equivalent to 1.85×10^{-3} μmol. Therefore,

$$\alpha_A \simeq \frac{32.6\,\mu\text{mol}}{1.85 \times 10^{-3}\,\mu\text{mol}\,\text{min}} = 1.76 \times 10^4\,\text{min}^{-1}.$$

β_A: From the data of Huber et al. (1975), we have $\beta_A \simeq 2.7 \times 10^4$ min^{-1}, whereas Martínez-Bilbao et al. (1991) gives $\beta_A \simeq 1.8 \times 10^4$ min^{-1}. We have taken the average of $\beta_A \simeq 2.15 \times 10^4$ min^{-1}.

K_L: The volume of one *E. coli* is $\sim 8.0 \times 10^{-16}$ liter and its mass is $\sim 1.7 \times 10^{-12}$ g to yield a density of 2.1×10^3 g/liter. The parameter K_L in our model corresponds to the parameter $K_{m,Lac}/\rho$ in Wong et al. (1997) model and the values and the units of these two parameters reported in this paper are $\rho = 3.0 \times 10^2$ g of dry cell weight per liter and $K_{m,Lac} = 1.4 \times 10^{-4}$ M, which gives

$$K_{m,Lac}/\rho = \frac{1.4 \times 10^{-4}}{3.0 \times 10^2} = 4.6 \times 10^{-7}\,\text{mol/g}.$$

To obtain an estimate for K_L in M, we can multiply this value by the density of the cell, which gives $K_L \simeq 9.7 \times 10^{-4}$ M, in agreement with the value of $1.4 \pm 0.3 \times 10^{-3}$ M estimated by Martínez-Bilbao et al. (1991). We have taken the latter value.

K_A: This parameter in our model corresponds to $K_{m,Allo}/\rho$ in the Wong et al. (1997) model, and they took $K_{m,Allo} \simeq 2.8 \times 10^{-4}$ M. Hence, $K_{m,Allo}/\rho = (2.8 \times 10^{-4})/\ (3.0 \times 10^2) = 9.3 \times 10^{-7}$ mol/g. Using the procedure followed in the estimation of K_L, the value of K_A is calculated to be 1.95 mM.

τ_M: In this model, we are considering the transcription and translation of two genes, *lacZ* and *lacY*. Translation of *lacZ* starts shortly after transcription initiation. For the translation of *lacY* to begin, *lacZ* must be completely transcribed. Knowing that *lacZ* has 1022 amino acids and DNA chain elongation rate is at least 490 nucleotides per second, which is equivalent to 9800 amino acids per minute, according to Bremmer and Dennis (1996), the time for *lacZ* to be completely transcribed is at most

$$\tau_M \simeq \frac{1022}{9800} = 0.1\,\text{min}.$$

This is an upper bound on τ_M.

τ_B: *lacZ* is 1022 amino acids long and the mRNA elongation rate varies between 12 and 33 amino acids per second (Monar et al., 1969; Kennell and Reizman, 1977). Talkad et al. (1976) also reported the translation rate is between 8 and 15 amino acids per second. If we take the mRNA elongation rate as 8 amino acids per second to estimate an upper bound value for τ_B, we obtain

$$\tau_B \simeq \frac{1022}{8 \times 60} = 2.12\,\text{min}.$$

If the elongation rate is 33 amino acids per second, then $\tau_B \simeq 1022/(33 \times 60) = 0.51$ min. Sorensen et al. (1989) estimated an average value for τ_B of 82 s experimentally, which is 1.37 min. We have taken the upper bound as $\tau_B \simeq 2.21$ min but used $\tau_B = 2.0$ min.

γ_L: We assumed $\gamma_L \simeq 0$, implying that the degradation rate for intracellular lactose is negligible when compared with the bacterial growth rate, as did Wong et al. (1997).

γ_P: West and Stein (1973) studied the kinetics of induction of β-galactosidase permease in *E. coli* and estimated the mean half life of permease ranges from 1.3 min to 1.9 min, which yields a range for 0.53–0.78 min^{-1} for the degradation rate of permease γ_P. We have taken an average of these two estimates to give $\gamma_P \simeq 0.65\,\text{min}^{-1}$.

α_L: Wright et al. (1981) studied on lactose carrier protein of *E. coli* and measured the active transport turnover number as $48 \times 60 = 2880$ min^{-1} in EDTA-treated cells of the strain ML308-225. We have taken the same value $\alpha_L = 2880$ min^{-1}.

α_P: Eq. 6 gives

$$\alpha_P = \frac{\bar{P}}{\bar{M}}\tilde{\gamma}_P e^{\mu(\tau_P + \tau_B)}$$

at a steady state. From Kennell and Reizman (1977), we know that $\bar{B}/\bar{M} \simeq 20$. The steady-state molar ratio of β-galactosidase to permease was given as $\bar{B}/\bar{P} = 2$ by in Maloney and Rotman (1973). >From this we estimate $\alpha_P \simeq 7.52\,\text{min}^{-1}$.

Lee and Bailey (1984) studied the growth rate effects on productivity of recombinant *E. coli* populations and obtained an empirical relation for the transcription rate as a function of the bacterial growth rate. From this relation, we have $\alpha_P = 17.37$ min^{-1} when $\mu = 2.21 \times 10^{-2}$ min^{-1}, which is the value we have estimated. We have taken an intermediate value between these two estimates: $\alpha_P \simeq 10.0\,\text{min}^{-1}$.

β_{L1}: From Wong et al. (1997), we have $\beta_{L1} = 2148$ min^{-1}. Lolkema et al. (1991) gave a range for β_{L1} as 840–3000 min^{-1}. We have chosen as $\beta_{L1} = 2650$ min^{-1}.

K_{L_e}: From Wong et al. (1997), we have

$$K_{L_e} = 2.6 \times 10^{-4}\,\mathrm{M},$$

based on the data of Lolkema et al. (1991), Huber et al. (1980), Page and West (1984), and Wright et al. (1981).

K_{L_1}: From Wong et al. (1997), we have

$$K_{L_1} = \frac{K_{t,lac}}{\rho},$$

wherein

$$K_{t,lac} = 2.6 \times 10^{-4}\,\mathrm{M}$$

from Lolkema et al. (1991), Huber et al. (1980), Page and West (1984), and Wright et al. (1981), and ρ is as given before. Thus

$$K_{L_1} = \frac{K_{t,lac}}{\rho} = 8.6 \times 10^{-7}\,\mathrm{mol/g}.$$

Multiplying by the density of the cell (2.1×10^3 gm/L) gives us

$$K_{L_1} = 1.81 \times 10^{-3}\,\mathrm{M}.$$

τ_P: *lacY* is 399 amino acids long and the mRNA elongation rate varies between 8 and 33 amino acids per second (Monar et al., 1969; Kennell and Reizman, 1977; and Talkad et al., (1976). If we take the mRNA elongation rate to be 8 amino acids per second to estimate an upper bound value for τ_P, we obtain

$$\tau_P \simeq \frac{399}{8 \times 60} = 0.83\,\mathrm{min}.$$

If the elongation rate is 33 amino acids per second, then $\tau_P \simeq 399/(33 \times 60) = 0.20\,\mathrm{min}$. We have taken the maximal value to be $\tau_P \simeq 0.83\,\mathrm{min}$.

APPENDIX C: STEADY-STATE ANALYSIS OF THE MODEL

In this section, the steady-state analysis of the system is investigated and a necessary condition derived for existence of positive steady state(s). Let $(\bar{M}, \bar{B}, \bar{A}, \bar{L}, \bar{P}) \in R_5^+$ be the steady state of the system given by Eqs. 2–6. At a steady state, by definition, there are no temporal changes and thus the steady state(s) are defined implicitly by

$$0 = \alpha_M f_1(\bar{A}) + \Gamma_0 - \tilde{\gamma}_M \bar{M} \tag{19}$$

$$0 = \alpha_{B_0} \bar{M} - \tilde{\gamma}_B \bar{B} \tag{20}$$

$$0 = \alpha_A g_1(\bar{L}) \bar{B} - \beta_A \bar{B} f_2(\bar{A}) - \tilde{\gamma}_A \bar{A} \tag{21}$$

$$0 = \alpha_L \bar{P} h - \beta_{L1} \bar{P} g_2(\bar{L}) - \beta_{L2} \bar{B} g_1(\bar{L}) - \tilde{\gamma}_L \bar{L} \tag{22}$$

$$0 = \alpha_{P_0} \bar{M} - \tilde{\gamma}_P \bar{P}, \tag{23}$$

where $\alpha_{B_0} = \alpha_B e^{-\mu\tau_B}$ and $\alpha_{P_0} = \alpha_P e^{-\mu(\tau_B + \tau_P)}$. Moreover, f_1, f_2, g_1, and g_2 are all monotone increasing functions given by

$$f_1(\bar{A}) = \frac{1 + K_1 E \bar{A}^2}{K_0 + K_1 E \bar{A}^2}, \quad f_2(\bar{A}) = \frac{\bar{A}}{K_A + \bar{A}} \tag{24}$$

$$g_1(\bar{L}) = \frac{\bar{L}}{K_L + \bar{L}}, \quad g_2(\bar{L}) = \frac{\bar{L}}{K_{L1} + \bar{L}}, \tag{25}$$

where $E = e^{-2\mu\tau_M}$.

For a steady state to make sense in a biological context, it is necessary that it be nonnegative. Now from Eqs. 20 and 23, we easily have

$$\bar{B} = \frac{\alpha_{B_0}}{\tilde{\gamma}_B} \bar{M} \tag{26}$$

$$\bar{P} = \frac{\alpha_{P_0}}{\tilde{\gamma}_P} \bar{M}. \tag{27}$$

Furthermore, from Eq. 19, $\bar{M}$ can be written in terms of $\bar{A}$ as,

$$\bar{M} = \frac{\alpha_M f_1(\bar{A}) + \Gamma_0}{\tilde{\gamma}_M}. \tag{28}$$

Note that $\bar{B}$ and $\bar{P}$ are nonnegative whenever $\bar{M}$ is nonnegative, and from Eq. 28 we always have $\bar{M} \geq 0$. Further, from Eq. 21 we can write $\bar{L}$ in terms of $\bar{A}$:

$$\bar{L}(\bar{A}) = \frac{K_L f_3(\bar{A})}{1 - f_3(\bar{A})}, \tag{29}$$

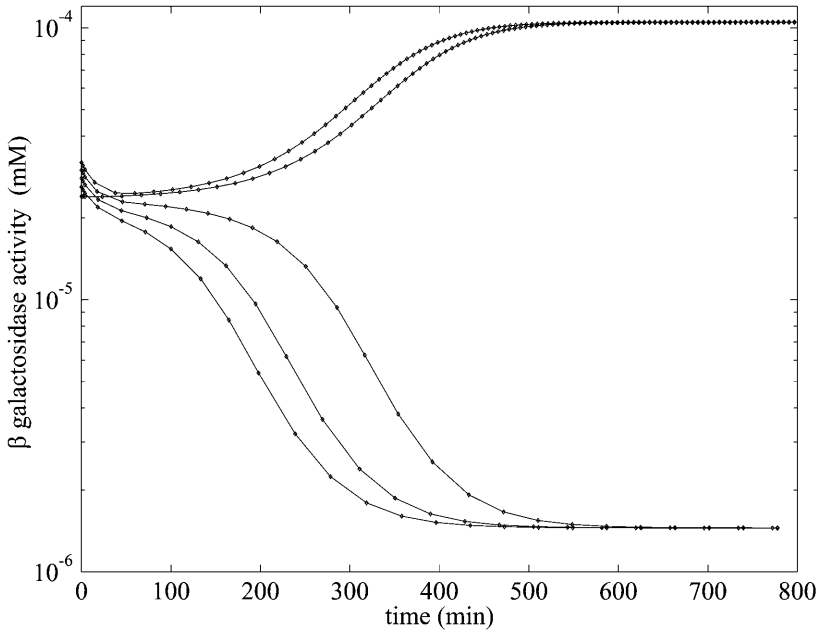

FIGURE 5 Semilog plot of β-galactosidase activity versus time (min) showing bifurcation in the numerical simulation with the parameters of Table 1 for five initial conditions and $\bar{\mu} \simeq 2.26 \times 10^{-2}\,\mathrm{min}^{-1}$ when $L_e = 3.0 \times 10^{-2}$ mM, which is in the range of lactose concentration for the existence of three steady states. The selection of the five initial conditions is described in the text.

TABLE 3 Multiple steady states and their numerical values when $L_e = 3.0 \times 10^{-2}$ mM

Steady states	$\bar{A}$	$\bar{M}$	$\bar{B}$	$\bar{L}$	$\bar{P}$
I	4.31×10^{-3}	2.14×10^{-6}	1.44×10^{-6}	1.01×10^{-1}	2.98×10^{-5}
II	6.43×10^{-2}	3.46×10^{-5}	2.34×10^{-5}	1.36×10^{-1}	4.83×10^{-4}
III	1.42×10^{-1}	1.54×10^{-4}	1.04×10^{-4}	1.39×10^{-1}	2.16×10^{-3}

where

$$f_3(\bar{A}) = \frac{\beta_A \alpha_{B_0} f_2(\bar{A})(\alpha_M f_1(\bar{A}) + \Gamma_0) + \tilde{\gamma}_A \tilde{\gamma}_M \tilde{\gamma}_B \bar{A}}{\alpha_A \alpha_{B_0}(\alpha_M f_1(\bar{A}) + \Gamma_0)}. \quad (30)$$

Condition I for a nonnegative steady state

From Eq. 29, to have a nonnegative steady-state value of $\bar{L}$,

$$0 \le f_3(\bar{A}) < 1 \quad (31)$$

must be satisfied.

Now consider Eq. 22, and substitute Eqs. 26 and 27. After rearrangement, we obtain

$$\alpha_M f_1(\bar{A}) + \Gamma_0 = \frac{\bar{L}\tilde{\gamma}_L}{\wp_1 - \wp_2 g_2(\bar{L}) - \wp_3 g_1(\bar{L})}, \quad (32)$$

where

$$\wp_1 = \frac{\alpha_L \alpha_{P_0} h}{\tilde{\gamma}_M \tilde{\gamma}_P} \quad (33)$$

$$\wp_2 = \frac{\beta_{L1} \alpha_{P0}}{\tilde{\gamma}_M \tilde{\gamma}_P} \quad (34)$$

$$\wp_3 = \frac{\beta_{L2} \alpha_{B_0}}{\tilde{\gamma}_M \tilde{\gamma}_B} \quad (35)$$

$$h = \frac{L_e}{K_L + L_e}. \quad (36)$$

The left side of Eq. 32 is always positive for all nonnegative values of $\bar{A}$, which leads to the following second condition for a biologically sensible steady state:

Condition II for a nonnegative steady state

Since the left side of Eq. 32 is always nonnegative, the condition

$$H_0(\bar{A}) = \wp_1 - \wp_2 g_2(\bar{L}(\bar{A})) - \wp_3 g_1(\bar{L}(\bar{A})) \ge 0, \quad (37)$$

must be satisfied.

Theorem 1

(Necessary condition for existence of a positive steady state.) For the existence of a positive steady state for the model given by Eqs. 2–6,

$$f_3'(\bar{A}) > 0 \quad (38)$$

is a necessary condition for $\bar{A}$ in an interval defined by the intersection of the intervals for which Eqs. 31 and 37 are satisfied.

Proof

The left side of Eq. 32 is a monotone increasing function of $\bar{A}$ when $K_1 > 0$, and has a minimal value of $(\alpha_M/K_0) + \Gamma_0$ when $\bar{A}=0$. Further, it reaches its maximal value of $\alpha_M + \Gamma_0$ as $\bar{A}$ becomes large. Furthermore, the right side

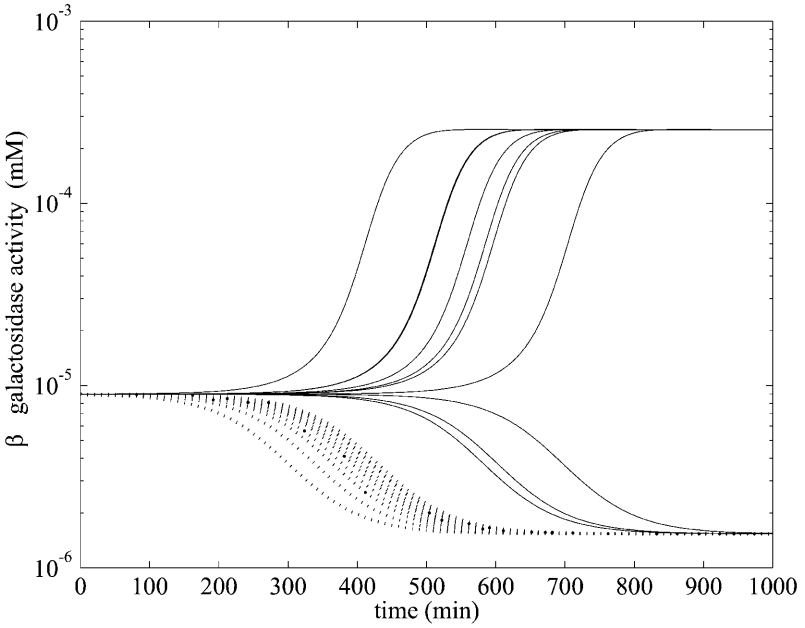

FIGURE 6 Semilog plot of β-galactosidase activity versus time showing effects of selection of the initial condition for $t \in [-\tau, 0]$ in the numerical simulation with the parameters of Table 1 and various initial values of mRNA and allolactose oscillating around the unstable steady-state values corresponding to the middle branch of Fig. 2 when $\bar{\mu} \simeq 2.26 \times 10^{-2}$ min^{-1} and $L_e = 4.0 \times 10^{-2}$ mM (which is in the range of lactose concentration for coexistence of three steady states). The solid lines show the β-galactosidase activity when the initial allolactose functions are $A(t) = \bar{A} + (\bar{A}/n)\sin(2\pi t/\tau_M)$ ($n = 1, 2, \ldots 10$), $t \in [-\tau_M, 0]$, and the other variables are at the steady-state values on the middle branch. (Here $\bar{A}$ is the unstable steady-state value of A on the *middle branch*). The dotted lines depict the temporal changes in β-galactosidase activity when $M(t) = \bar{M} + (\bar{M}/n)\sin(2\pi t/(\tau_B + \tau_P))$ ($n = 1, 2, \ldots 10$) for $t \in [-(\tau_B + \tau_P), 0]$. Again all the other variables are at the steady-state values when $L_e = 4.0 \times 10^{-2}$ mM and $\bar{M}$ is also the steady-state value of A on the middle branch. The steady-state values are $\bar{A} = 3.75 \times 10^{-2}$ mM, $\bar{M} = 1.32 \times 10^{-5}$ mM, $\bar{B} = 8.97 \times 10^{-6}$ mM, $\bar{L} = 1.74 \times 10^{-1}$ mM, and $\bar{P} = 1.84 \times 10^{-4}$ mM, when $L_e = 4.0 \times 10^{-2}$ mM.

of Eq. 32 is zero when $\bar{A}=0$. Therefore, for the existence of a positive root, it is trivial that the right of Eq. 32 must be an increasing function of $\bar{A}$ for values of $\bar{A}$ and $\bar{L}$ satisfying Eqs. 31 and 37.

To prove that the condition $f_3'(\bar{A})>0$ is a necessary condition for the right side of Eq. 32 to be an increasing function of $\bar{A}$, let

$$H_1(\bar{A})=\frac{\bar{L}\widetilde{\gamma}_L}{\wp_1-\wp_2 g_2(\bar{L})-\wp_3 g_1(\bar{L})} \tag{39}$$

so that

$$\frac{dH_1(\bar{A})}{d\bar{A}}=\frac{\bar{L}'\widetilde{\gamma}_L\{H_0(\bar{A})+\bar{L}(\wp_2 g_2'(\bar{L})+\wp_3 g_1'(\bar{L}))\}}{H_0(\bar{A})^2}. \tag{40}$$

$g_1(\bar{A})$ and $g_2(\bar{A})$ are Michaelis-Menten type functions and $g_1'(\bar{L})$ and $g_2'(\bar{L})$ are positive. Since $H_0(\bar{A})>0$ the condition

$$\frac{dH_1(\bar{A})}{d\bar{A}}>0$$

is satisfied whenever

$$\bar{L}'\equiv\frac{d\bar{L}}{d\bar{A}}>0$$

holds.

Further, from Eq. 29 we have

$$\frac{d\bar{L}}{d\bar{A}}=\frac{K_L f_3(\bar{A})(1-f_3(\bar{A}))+f_3'(\bar{A})K_L f_3(\bar{A})}{(1-f_3(\bar{A}))^2}, \tag{41}$$

and from Condition I, $1-f_3(\bar{A})>0$ must be satisfied for nonnegative steady states. Thus the right side of Eq. 41 is always positive when $f_3'(\bar{A})>0$. Therefore, $H_1(\bar{A})$ is an increasing function when $f_3'(\bar{A})>0$ in an interval defined by the intersection of the intervals for which Eqs. 31 and 37 are satisfied. This completes the proof.

APPENDIX D: NUMERICAL STABILITY OF THE MODEL

A full stability analysis of the steady states of this model is impossible, since the eigenvalue equation determining local stability is a fifth order quasi-polynomial containing three delays. Consequently, we have contented ourselves with a numerical examination of the stability properties of the steady states.

Briefly, the results of our numerical stimulations are as follows. When a single steady state exists, we have found that the numerical behavior is such that the model solutions always converge to that steady state at large times.

When there are three coexisting steady states as illustrated in Fig. 2, the behavior is slightly more complicated and is illustrated in Fig. 5 when $L_e=3.0\times10^{-2}$. At this value, the system has the three steady states given in Table 3. As seen from the results in Fig. 5, the numerical model solutions either converged to the lower or upper branch of the *S*-shaped curve (see Fig. 2) for various initial conditions. These results, as well as numerous others that are not shown, lead us to conclude that the middle branch of the *S*-shaped steady-state curve corresponds to a steady state that is globally unstable.

For this simulation, we choose five equally distributed initial β-galactosidase levels between 0.24×10^{-4} and 0.32×10^{-4} mM and kept all other variables at their steady-state values corresponding to the values on the middle branch of the *S*-shaped curve in Fig. 2 when $L_e=3.0\times10^{-2}$ mM, and computed the temporal evolution of the model variables. For initial β-galactosidase values equal to or greater than 3.0×10^{-5}, the simulated curves converged to 1.04×10^{-4}, which is the value on the upper branch of the steady-state curve, whereas for the other initial values, the β-galactosidase values converged to 1.44×10^{-6}, which is the steady-state value on the lower branch.

However, the relatively simple behavior shown in Fig. 5 is deceptive, as shown in Fig. 6. There we present numerical evidence that the attractor boundary in initial function space separating behaviors where one approaches the lower or upper locally stable steady state of Fig. 2 is not totally straightforward. The potentially rich nature of the boundary is revealed by taking initial functions that oscillate about the unstable branch of the steady-state curve. The ensuing dynamical behavior is highly reminiscent of the existence of a fractal basin boundary that has been noted in other, simpler, differential delay systems (Losson and Mackey, 1993).

We thank Dr. Photini Pitsikas for her initial suggestion of this problem, Profs. Claire Cupples and Moisés Santillán for their advice on parameter estimation and general comments, and Mr. Daisuke Horike for many helpful discussions.

This work was supported by the Scientific and Technical Research Council of Turkey, the North Atlantic Treaty Organization, the Mathematics of Information Technology and Complex Systems (Canada), the Natural Sciences and Engineering Research Council (grant OGP-0036920, Canada), Le Fonds pour la Formation de Chercheurs et l'Aide à la Recherche (grant 98ER1057, Québec), and the Leverhulme Trust (UK).

REFERENCES

Arkin, A., J. Ross, and H. H. McAdams. 1998. Stochastic kinetic analysis of developmental pathway bifurcation in phage λ-infected *Escherichia coli* cells. *Genetics*. 149:1633–1648.

Baneyx, F. 1999. Recombinant protein expression in *Escherichia coli*. *Curr. Opin. Biotechnol.* 10:411–421.

Beckwith, J. 1987a. The lactose operon. *In* Escherichia coli and Salmonella: Cellular and Molecular Biology, Vol. 2. F. C. Neidhardt, J. L. Ingraham, K. B. Low, B. Magasanik, and H. E. Umbarger, editors. American Society for Microbiology, Washington, DC. 1444–1452.

Beckwith, J. 1987b. The operon: An historical account. *In* Escherichia coli and Salmonella: Cellular and Molecular Biology, Vol. 2. F. C. Neidhardt, J. L. Ingraham, K. B. Low, B. Magasanik, and H. E. Umbarger, editors. American Society for Microbiology, Washington, DC. 1439–1443.

Bliss, R. D., R. P. Painter, and A. G. Marr. 1982. Role of feedback inhibition in stabilizing the classical operon. *J. Theor. Biol.* 97:177–193.

Blundell, M., and D. Kennell. 1974. Evidence for endonucleolytic attack in decay of *lac* messenger RNA in *Escherichia coli*. *J. Mol. Biol.* 83: 143–161.

Bremmer, H., and P. P. Dennis. 1996. Modulation of chemical composition and other parameters of the cell by growth rate. *In* Escherichia coli and Salmonella: Cellular and Molecular Biology, Vol. 2. F. C. Neidhardt, R. Curtiss, J. L. Ingraham, E. C. C. Lin, K. B. Low, B. Magasanik, W. S. Reznikoff, M. Riley, M. Schaechter, and H. E. Umbarger, editors. American Society for Microbiology, Washington, DC. 1553–1569.

Cohn, M., and K. Horibata. 1959. Inhibition by glucose of the induced synthesis of the β-galactosidase-enzyme system of *Escherichia coli*: analysis of maintenance. *J. Bacteriol.* 78:613–623.

Gillespie, D. T. 1977. Exact stochastic simulation of coupled chemical reactions. *J. Phys. Chem.* 81:2340–2361.

Gillespie, D. T. 1992. A rigorous derivation of the chemical master equation. *Physica A*. 188:404–425.

Goodwin, B. 1965. Oscillatory behaviour in enzymatic control process. *Adv. Enz. Regul.* 3:425–438.

Goodwin, B. C. 1969. Control dynamics of β-galactosidase in relation to the bacterial cell cycle. *Eur. J. Biochem.* 10:515–522.

Griffith, J. S. 1968a. Mathematics of cellular control processes. I. Negative feedback to one gene. *J. Theor. Biol.* 20:202–208.

Griffith, J. S. 1968b. Mathematics of cellular control processes. II. Positive feedback to one gene. *J. Theor. Biol.* 20:209–216.

Huber, R. E., M. Gupta, and S. Khare. 1994. The active site and mechanism of the β-galactosidase from *Escherichia coli*. *Int. J. Biochem.* 26: 309–318.

Huber, R. E., G. Kurz, and K. Wallenfels. 1976. A quantitation of the factors which affect the hydrolase and transgalactosylase activities of β-galactosidase (*E. coli*) on lactose. *Biochemistry.* 15:1994–2001.

Huber, R., R. Pisko-Dubienski, and K. Hurlburt. 1980. Immediate stoichiometric appearance of β-galactosidase products in the medium of *Escherichia coli* cells incubated with lactose. *Biochem. Biophys. Res. Commun.* 96:656–661.

Huber, R. E., W. Wallenfels, and G. Kurz. 1975. The action of β-galactosidase *Escherichia coli* on allolactose. *Can. J. Biochem.* 53:1035–1039.

Jacob, F., D. Perrin, C. Sanchez, and J. Monod. 1960. L'operon: groupe de gène à expression par un operatour. *C. R. Acad. Sci.* 250:1727–1729.

Ji-Fa, J. 1994. A Liapunov function for four dimensional positive feedback systems. *Quar. Appl. Math.* 52:601–614.

Kennell, D., and H. Reizman. 1977. Transcription and translation initiation frequencies of the *Escherichia coli* lac operon. *J. Mol. Biol.* 114:1–21.

Kepler, T. B., and T. C. Elston. 2001. Stochasticity in transcriptional regulation: origins, consequences, and mathematical representations. *Biophys. J.* 81:3116–3136.

Knorre, W. A. 1968. Oscillation of the rate of synthesis of β-galactosidase in *Escherichia coli* ML 30 and ML 308. *Biochem. Biophys. Res. Commun.* 31:812–817.

Lee, S. B., and J. E. Bailey. 1984. Analysis of growth rate effects on productivity of recombinant *Escherichia coli* populations using molecular mechanism models. *Biotechnol. Bioeng.* 67:805–812.

Leive, L., and V. Kollin. 1967. Synthesis, utilization and degradation of lactose operon mRNA in *Escherichia coli*. *J. Mol. Biol.* 24:247–259.

Lolkema, J., N. Carrasco, and H. Kaback. 1991. Kinetic analysis of lactose exchange in proteoliposomes reconstituted with purified *lac* permease. *Biochemistry.* 30:1284–1290.

Losson, L., and M. C. Mackey. 1993. Solution multistability in first order nonlinear differential delay equations. *Chaos.* 3:167–176.

Maffahy, J. M., and E. Savev. 1999. Stability analysis for a mathematical model of the *lac* operon. *Quar. Appl. Math.* 57:37–53.

Maloney, P. C., and S. M. Rotman. 1973. Distribution of suboptimally induced β-D-galactosidase in *Escherichia coli*. *J. Mol. Biol.* 73: 77–91.

Mandelstam, J. 1957. Turnover of protein in starved bacteria and its relationship to the induced synthesis of enzyme. *Nature.* 179:1179–1181.

Martínez-Bilbao, M., R. E. Holdswards, L. A. Edwards, and R. E. Huber. 1991. A highly reactive β-galactosidase *Escherichia coli* resulting from a substitution of an aspartic acid for Gly-794. *J. Biol. Chem.* 266:4979–4986.

McAdams, H. H., and L. Shapiro. 1995. Circuit simulation of genetic networks. *Science.* 269:650–656.

Monar, H., D. Goodman, and G. S. Stnet. 1969. RNA chain growth rates in *Escherichia coli*. *J. Mol. Biol.* 39:1–29.

Novick, A., and M. Wiener. 1957. Enzyme induction as an all-or-none phenomenon. *Proc. Natl. Acad. Sci. USA.* 43:553–566.

Osumi, T., and M. H. Saier. 1982. Regulation of lactose permease activity by the phosphoenolpyruvate: sugar phosphotransferase system: Evidence for direct binding of the glucose specific enzyme III to the lactose permease. *Proc. Natl. Acad. Sci. USA.* 79:1457–1461.

Page, M. G. P., and I. C. West. 1984. The transient kinetics of uptake of galactosides into *Escherichia coli*. *Biochem. J.* 223:723–731.

Pestka, S., B. L. Daugherty, V. Jung, K. Hotta, and R. K. Pestka. 1984. Anti-mRNA: specific inhibition of translation of single mRNA molecules. *Proc. Natl. Acad. Sci. USA.* 81:7525–7528.

Postma, P. W., J. W. Lengeler, and G. R. Jacobson. 1996. Phosphoenolpyruvate-carbohydrate phosphotransferase systems. *In* Escherichia coli and Salmonella: Cellular and Molecular Biology, Vol. 1. F. C. Neidhart, R. Curtiss, J. L. Ingraham, E. C. C. Lin, K. B. Low, B. Magasanik, W. S. Reznikoff, M. Riley, M. Schaechter, and H. E. Umbarger, editors. American Society for Microbiology, Washington, DC. 1149–1174.

Rotman, R., and S. Spiegelman. 1954. On the origin of the carbon in induced synthesis of β-galactosidase. *J. Bacteriol.* 68:419–429.

Saier Jr., M. H. 1976. Inducer exclusion and regulation of the melibose, maltose, glycerol, and lactose transport systems by the phosphoenolpyruvate: sugar phosphotransferase system. *J. Biol. Chem.* 251: 6606–6615.

Saier, M. H., T. M. Ramseier, and J. Reizer. 1996. Regulation of carbon utilization. *In* Escherichia coli and Salmonella: Cellular and Molecular Biology, Vol. 1. F. C. Neidhardt, R. Curtiss, J. L. Ingraham, E. C. C. Lin, K. B. Low, B. Magasanik, W. S. Reznikoff, M. Riley, M. Schaechter, and H. E. Umbarger, editors. American Society for Microbiology, Washington, DC. 1325–1343.

Santillán, M., and M. C. Mackey. 2001a. Dynamic behaviour in mathematical models of the tryptophan operon. *Chaos.* 11:261–268.

Santillán, M., and M. C. Mackey. 2001b. Dynamic regulation of the tryptophan operon: a modeling study and comparison with experimental data. *Proc. Natl. Acad. Sci. USA.* 98:1364–1369.

Savageau, M. A. 1999. Design of gene circuitry by natural selection: analysis of the lactose catabolic system in *Escherichia coli*. *Biochem. Soc. Trans.* 27:264–270.

Selgrade, J. F. 1979. Mathematical analysis of a cellular control process with positive feedback. *SIAM J. Appl. Math.* 36:219–229.

Selgrade, J. F. 1982. A Hopf bifurcation in single loop positive feedback systems. *Quar. Appl. Math.* 40:347–351.

Sen, A. K., and W. Liu. 1989. Dynamic analysis of genetic control and regulation of amino acid synthesis: the tryptophan operon in *Escherichia coli*. *Biotechnol. Bioeng.* 35:185–194.

Shampine, L. F., and S. Thompson. 2000. Solving DDEs with MATLAB. www.radford.edu/~thompson/webddes/.

Sinha, S. 1988. Theoretical study of tryptophan operon: application in microbial technology. *Biotechnol. Bioeng.* 31:117–124.

Sorensen, M. A., C. G. Kurland, and S. Pedersen. 1989. Codon usage determines translation rate in *Escherichia coli*. *J. Mol. Biol.* 207:365–377.

Swain, P. S., M. Elowitz, and E. Siggia. 2002. Intrinsic and extrinsic contributions to stochasticity in gene expression. *Proc. Natl. Acad. Sci. USA.* 99:12795–12800.

Talkad, V., E. Schneider, and D. Kennell. 1976. Evidence for variable rates of ribosome movement in *Escherichia coli*. *J. Mol. Biol.* 104:299–303.

Tyson, J. J., and M. C. Mackey. 2001. Molecular, metabolic and genetic control: An introduction. *Chaos.* 11:81–83.

Tyson, J. J., and H. G. Othmer. 1978. The dynamics of feedback control circuits in biochemical pathways. *In* Progress in Biophysics, Vol. 5. R. Rosen, editor. Academic Press, New York. 1–62.

Watson, J. D. 1977. Molecular Biology of the Gene, 3rd ed. W. A. Benjamin, New York.

West, I. C., and W. D. Stein. 1973. The kinetics of induction of β-galactoside permease. *Biochim. Biophys. Acta.* 308:161–167.

Wong, P., S. Gladney, and J. D. Keasling. 1997. Mathematical model of the *lac* operon: inducer exclusion, catabolite repression, and diauxic growth on glucose and lactose. *Biotechnol. Prog.* 13:132–143.

Wright, J. K., I. Riede, and P. Overath. 1981. Lactose carrier protein of *Escherichia coli*: interaction with galactosides and protons. *Biochemistry.* 20:6404–6415.

Xiu, Z. L., A. P. Zeng, and W. D. Deckwer. 1997. Model analysis concerning the effects of growth rate and intracellular tryptophan level on the stability and dynamics of tryptophan biosynthesis in bacteria. *J. Biotech.* 58:125–140.

Yagil, G., and E. Yagil. 1971. On the relation between effector concentration and the rate of induced enzyme synthesis. *Biophys. J.* 11:11–27.